Korean J. Chem. Eng., **20**(4), 617-623 (2003)

Optimal Operation of the Pressure Swing Adsorption (PSA) Process for CO_2 Recovery

Wan-Kyu Choi*, Tae-In Kwon, Yeong-Koo Yeo†, Hwaung Lee, Hyung Keun Song** and Byung-Ki Na*****

Department of Chemical Engineering, Hanyang University, Seoul 133-791, Korea
*Honam Petrochemical Co., Ltd., Yeocheon, Chunnam 555-805, Korea
**Korea Institute of Science and Technology, Seoul 136-791, Korea
***Dept. of Chemical Eng., Chungbuk National Univ., Chungbuk 361-763, Korea
(*Received 21 October 2002 • accepted 19 February 2003*)

Abstract−The operation of PSA (Pressure Swing Adsorption) processes is a highly nonlinear and challenging problem. We propose a systematic procedure to achieve the optimal operation of a PSA process. The model of the PSA process for CO_2 separation and recovery is developed first and optimization is performed to identify optimal operating conditions based on the model. The effectiveness of the model developed is demonstrated by numerical simulations and experiments using CO_2 and N_2 gases and zeolite 13X. Breakthrough curves and temperature changes in the bed are computed from the model and the results are compared with those of experiments. The effects of the adsorption time and reflux ratio on the product purity and the recovery are identified through numerical simulations. The optimization problem is formulated based on nonlinear equations obtained from simulations. The optimal operating conditions identified are applied to experiments. The results show higher recovery of CO_2 under optimal operating conditions.

Key words: PSA, Modeling, Separation, SQP, Optimization

INTRODUCTION

Modern industry consumes a huge amount of fossil fuel that causes inevitable CO_2 exhaust. For example, the flue gas from iron or cement industry contains 20-30% of CO_2 by volume and the concentration of CO_2 of the flue gas from a typical electric power plant is about 16%. Increase of CO_2 concentration in the atmosphere gives rise to severe environmental problems such as the green house effect. Therefore reduction of CO_2 has been one of the hottest research areas and many results have been published concerning ways decreasing CO_2 exhaust, the techniques of CO_2 recovery, the method of using and freezing CO_2 and the alternative energy sources which do not generate CO_2. Among these CO_2 recovery has been the most active research field and various CO_2 recovery techniques have been reported. PSA (Pressure Swing Adsorption) is well known as one of the most promising methods to recover CO_2 [Kikkinides et al., 1993; Chue et al., 1995; Kim et al., 1998]. Utilization of the PSA technique in the removal and recovery of SO_x, NO_x and other materials and in the purification of gaseous products can be found elsewhere [Na and Eum, 2001; Kikkinides et al., 1991; Moon et al., 1986; Kim et al., 1992; Suzuki, 1990; Yang and Doong, 1985; Yang et al., 1998]. The present study aims at the development of an optimal operation system for the PSA process for CO_2 separation and recovery experimentally and theoretically.

So far large-scale PSA processes have been preferred over small-scale ones because the PSA for high CO_2 concentration is more economical. The PSA for low CO_2 concentration had some problems concerning efficient CO_2 recovery. In this work, we focus on the optimal operation of a PSA process to recover low concentration CO_2 from flue gas to overcome difficulties in efficient CO_2 recovery.

†To whom correspondence should be addressed.
E-mail: ykyeo@hanyang.ac.kr

Effects of the adsorbent, the ambient temperature and the desorption pressure on the PSA performance have been studied by many researchers. But, the effect of the adsorption time to determine operating time and the effect of reflux ratio on the rinse step in the operating steps has attracted little attention. In the present study, effects of these variables on the product purity and on the performance of recovery were identified through simulations. Furthermore, optimal operating conditions for the maximum recovery of CO_2 by the PSA process were investigated both theoretically and experimentally. Dynamic modeling and cyclic steady state modeling of the PSA process based on experimental results were performed. Comparison between results of numerical simulations and those of experiments demonstrated the effectiveness of the model developed in the present work.

EXPERIMENTS

The experimental units mainly consist of three adsorption beds, gas reservoirs and a measurement unit as shown in Fig. 1. Each bed is 900 mm length and 41.2 mm diameter. A vacuum pump is used in the evacuative desorption step, and a back pressure regulator (BPR, TESCOM) is used to control the adsorption pressure in the beds. A pressure transmitter (PT) is employed to display pressure in the beds and 4 thermocouples in each bed measure temperature changes at process steps. The solenoid valves control the gas flow rates via the programmable logic controller (PLC, Siemens Simatic S5-95U). The wet test meter (Sinagawa Co, Japan) is used to measure the final product flow rate and the gas chromatography (GC, HP5890) is employed to measure the final product concentration.

Zeolite 13X was used as the adsorbent. Physical properties of Zeolite 13X are listed in Table 1. The target gas of the present study is the flue gas from thermoelectric power plants. The real flue gas consists of 5-6% H_2O and less than 1% SO_2, NO_x, and the compo-

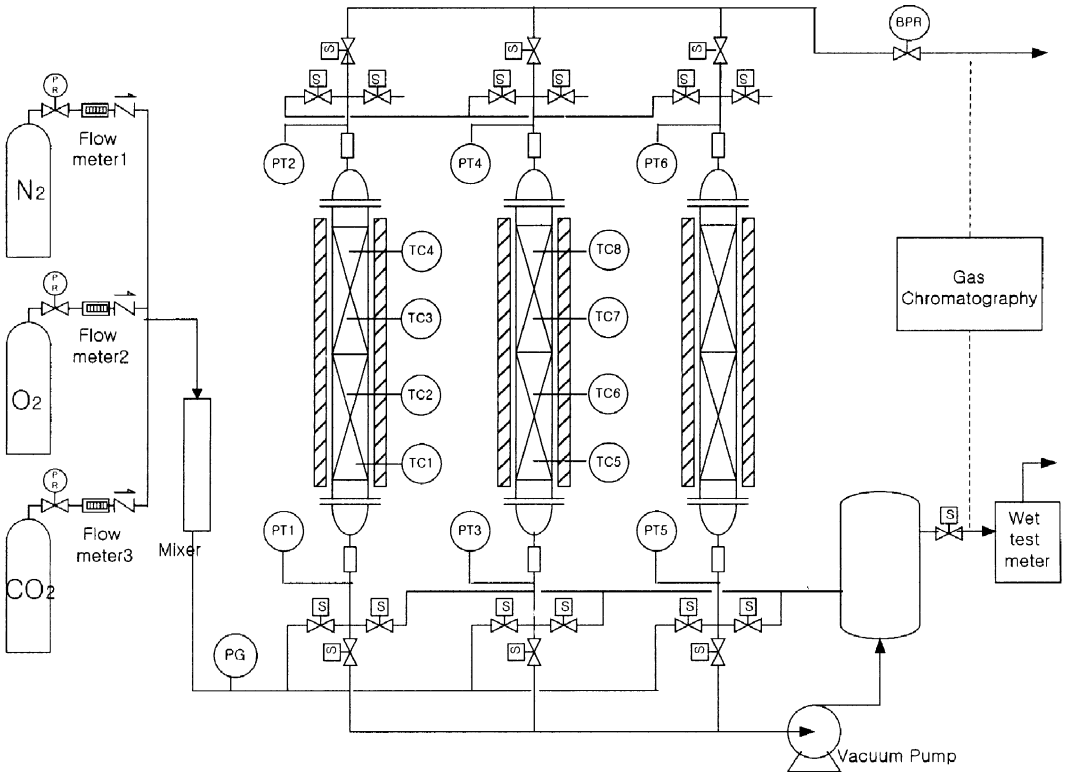

Fig. 1. Experimental units for 3-bed PSA process.

Table 1. Physical properties of the adsorbent

Adsorbent	Zeolite 13X
Particle size (mesh)	8-12
Bed bulk density (kg/m^3)	0.70
BET area (m^2/g)	614
Total pore volume (cm^3/g)	0.4
Average pore diameter (Å)	19

Table 2. Operating conditions

Bed length (mm)	900
Volume of adsorbent (cm^3)	1200
Feed flow rate (LPM)	10.0
Feed composition (%)	CO_2 13, N_2 83, O_2 4
Pressure ($P_{adsorption}/P_{rinse}/P_{evacuation}$, atm)	1.5/1.0/0.05

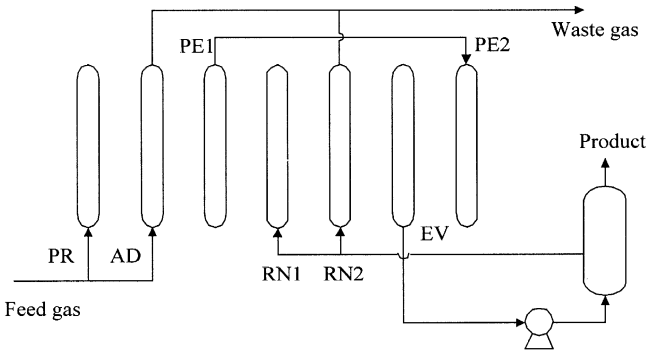

PR	AD	PE1	RN1	RN2		EV		PE2
RN1	RN2		EV		PE2	PR	AD	PE1
EV		PE2	PR	AD	PE1	RN1	RN2	

Fig. 2. PSA operation schedule.

PR pressurization step (with feed)
AD adsorption step
PE1 pressure equalization step (co-current)
PE2 pressure equalization (counter-current)
RN1 pressurization step (with product)
RN2 rinse step step
PD product withdrawal step
EV evacuation step

sition of the feed gas is 13% CO_2, 83% N_2, and 4% O_2. In the experiments we made a gas mixture the composition of which is the same as the feed gas. Feed flow rate was set to be 10 LPM, and the pressure of the adsorption step was maintained at 1.5 atm. The pressure of rinse step for higher product purity was atmospheric pressure, and the pressure of the desorption step for the regeneration of the adsorbent was 0.05 atm. Operating conditions are summarized in Table 2.

In order to separate and to recover more strongly adsorbed species, the process cycle consisted of pressurization step, adsorption step, pressure equalization step, rinse step, and evacuation step for the desorption. The operation sequence of the experimental apparatus is shown in Fig. 2. At the pressurization step, the feed gas is fed to the bed inlet while the bed outlet is closed. When the pressure in the bed reaches to 1.5 atm, the bed outlet is opened followed by the adsorption step. The adsorption step is then followed by the pressure equalization step. At this step, the bed at the end of the adsorption

step is connected to other bed at the end of evacuation step through their outlets. Therefore, the energy cost for pressurization and blow-down can be reduced by the pressure equalization step, which is followed by the rinse step. At the rinse step, part of the product flow is recycled to the beds to increase the product purity. Part of the adsorbate in the pore is removed and even a small quantity of less strong adsorbate in the adsorbent is replaced with more strong adsorbate. To operate the rinse step at the atmospheric pressure, the adsorption bed of which the pressure is below atmospheric pressure due to pressure equalization step is pressurized by part of the product gas. Thus the rinse step was divided by the variable pressure step and the constant pressure step.

MODELING AND SIMULATION OF THE PSA PROCESS

In the modeling of the PSA process, mass transfer equations, mass balances, energy balances and the equilibrium adsorption isotherm should be considered. Many researchers presented results on the modeling of PSA processes [Ragahaven and Ruthven, 1985; Farooq and Ruthven, 1991]. In the present study the following assumptions were employed:

- The gas flow rate in the bed is mainly affected by the bed height and the residence time.
- The axial diffusion effect is ignored.
- The radial diffusion effect is ignored because of the short bed radius compared to the bed length.
- The pressure is constant in the bed at adsorption step and rinse step, which means the pressure drop can be ignored.
- Extended Langmuir isotherm model is employed as the equilibrium adsorption isotherm.
- LDF (Linear driving force) model is adopted as the mass transfer equation.
- The gas in the bulk phase is considered as the ideal gas.
- The process is considered as a binary system of CO_2 and N_2 because of the similar adsorption properties of O_2 with N_2.
- The process is considered as an adiabatic system.

Based on these assumptions we can write the mass balance for each component and the total mass balance as

$$\frac{\partial C_i}{\partial t} + u\frac{\partial C_i}{\partial z} + C_i\frac{\partial u}{\partial z} + \frac{\rho_{bulk}}{\varepsilon}\frac{\partial q_i}{\partial t} = 0, \quad i=1, \ldots, n \tag{1}$$

$$\frac{\partial (uC_{total})}{\partial z} + \frac{\partial C_{total}}{\partial t} + \frac{\rho_{bulk}}{\varepsilon}\sum_{i=1}^{n}\frac{\partial q_i}{\partial t} = 0 \tag{2}$$

where C_{total} is $\sum_{i=1}^{n} C_i$, C_i and q_i is concentrations of i in the gas and the adsorption phase, respectively; u is the velocity, ρ_{bulk} is the bulk density and ε is the voidage.

The mass transfer equation in the gas and adsorption phases is given by

$$\frac{\partial q_i}{\partial t} = k_i(q_i^* - q_i) \tag{3}$$

where k_i is the mass transfer coefficient. q_i^* is the amount of equilibrium adsorption which can be written as

$$q_i^* = \frac{q_{mi} b_i P_i}{1 + \sum_{j=1}^{n} b_j P_j} \tag{4}$$

where q_m and b are Langmuir parameters both of which are functions of temperature as given by

$$q_m = t_1 + t_2 T \tag{5}$$

$$b = t_3 \exp(t_4/T) \tag{6}$$

where t_1, t_2, t_3, t_4 are calculated by adsorption isotherm experiments by using pure CO_2 and N_2 gases and zeolite 13X. Values of t_1, t_2, t_3, t_4 are shown in Table 3.

The energy balance can be represented as

$$(\varepsilon\rho_g C_{pg} + \rho_{bulk} C_s)\frac{\partial T}{\partial t} + (\varepsilon\rho_g C_{pg})u\frac{\partial T}{\partial z} + \rho_{bulk}\sum_{j=1}^{n}\frac{\partial q_j}{\partial t}\Delta H_j = 0 \tag{7}$$

where C_{pg} and C_s are heat capacities of the gas and the adsorbent, respectively, ρ_g is the density of the gas mixture and ΔH_j is the heat of adsorption for each component. The heat of adsorption is isosteric heat and can be calculated by Clausius-Clapeyron equation as

$$\left[\frac{d\ln P}{d\left(\frac{1}{T}\right)}\right]_q = -\frac{\Delta H}{R_g} \tag{8}$$

Typical data used in the modeling are listed in Table 4. The mass transfer coefficient is the tuning parameter which can be acquired by breakthrough experiments. To solve partial differential equations in the modeling equations we need suitable initial and boundary conditions. Computational results of one step become initial or boundary conditions for the next step. Boundary conditions are summarized in Table 5. In Table 5, (+) means the same direction as the feed flow and (−) means the opposite direction to the feed.

Table 3. Parameters of extended Langmuir isotherm of zeolite 13X

Gas	t_1 (mmol/g)	t_2 (mmol/g K)	t_3 (atm^{-1})	(K)
CO_2	10.220	−0.0206	0.10254	1567.056
N_2	15.547	−0.0446	0.00172	1339.168

IDENTIFICATION OF THE OPTIMAL OPERATING CONDITIONS

In the PSA process the input variables consist of the adsorption

Table 4. Typical modeling data

Heat of adsorption, ΔH ($Jmol^{-1}$)	CO_2	4.7827×10^3
	N_2	3.3591×10^3
Heat capacity of gas, C_{pg} ($Jg^{-1}K^{-1}$)		0.9942
Heat capacity of adsorbent, C_{ps} ($Jg^{-1}K^{-1}$)		0.920
Bed voidage, ε (-)		0.348
Mass transfer coefficient, k_i (s^{-1})	CO_2	0.10
	N_2	0.01

Table 5. Boundary conditions for each step

Step	Direction	Concentration	Temperature	Pressure	Velocity
Pressurization (PR)	(+)	$y_i(t, 0)=y_{f,i}$	$T(t, 0)=T_0$	$P=P(t)$	$u(t, L)=0$
Adsorption (AD)	(+)	$y_i(t, 0)=y_{f,i}$	$T(t, 0)=T_0$	$P=P_H$	$u(t, 0)=u_{feed}$
Evacuation (EV)	(−)			$P=P(t)$	$u(t, L)=0$
Pressure equalization (PE1, PE2)	(+)	$y_i(t, L)=y_{Eq}$	$T(t, L)=T_{Eq}$	$P=P(t)$	$u(t, L)=0$
	(−)	$y_i(t, L)=y_{Eq}$	$T(t, L)=T_{Eq}$	$P=P(t)$	$u(t, 0)=0$
Rinse (RN1, RN2)	(+)	$y_i(t, 0)=y_{product}$	$T(t, 0)=T_{Ev}$	$P=P(t)$	$u(t, L)=0$
	(+)	$y_i(t, 0)=y_{product}$	$T(t, 0)=T_{Ev}$	$P=P_L$	$u(t, 0)=u_{RN}$

pressure, the desorption pressure, the feed flow rate, the adsorption step time and the reflux ratio for rinse step. Output variables consist of product purity, recovery and productivity. The optimization problem is formulated in terms of these variables as well as constraints. The adsorption step time and the reflux ratio for the rinse step were chosen as input variables upon which the product purity and the recovery are dependent. The primary objective of the optimization in the present study is to maximize CO_2 recovery. Therefore, the CO_2 recovery itself becomes the main objective function in the optimization. Constraints in the optimization problem can be summarized as:

(1) CO_2 purity of the product should be higher than 90% (or 95%).
(2) The reflux ratio for the rinse step lies in the range of 0.78-0.90.
(3) The adsorption step time is within the range of 200-600 sec.

In addition to these, nonlinear equations representing the product purity and the recovery were added as inequality constraints. MATLAB was employed to solve the optimization problem. A MATLAB function based on sequential quadratic programming (SQP) method was used to solve the constrained nonlinear programming optimization problem.

RESULTS AND DISCUSSIONS

1. Simulations and Experiments

For the PSA processes we can say that there are cyclic steady states. In the simulations, the PSA process appeared to retain almost the same features after about 10 cycles. This fact means that the cyclic steady state is achieved after 10 cycles of operation.

First, the concentration changes of CO_2 at the product end of the adsorption bed were analyzed. From the analysis we obtained a so-called breakthrough curve. The breakthrough curve of the cyclic steady state was different from that of initial state. In other words, the regenerating step of the adsorbent was not performed perfectly by the desorption step, and small amount of CO_2 gas remained in the adsorbent. Results of simulations were compared with those of experiments in terms of the breakthrough curve of the cyclic steady state as shown in Fig. 3. Concentration changes of CO_2 at the product end of the adsorption bed were plotted at the cyclic steady state when the adsorption step time was 600 sec. In Fig. 3, we can see that simulation results show good agreement with experimental results. Fig. 3 indicates that the control of the adsorption step time is very important to increase the product recovery.

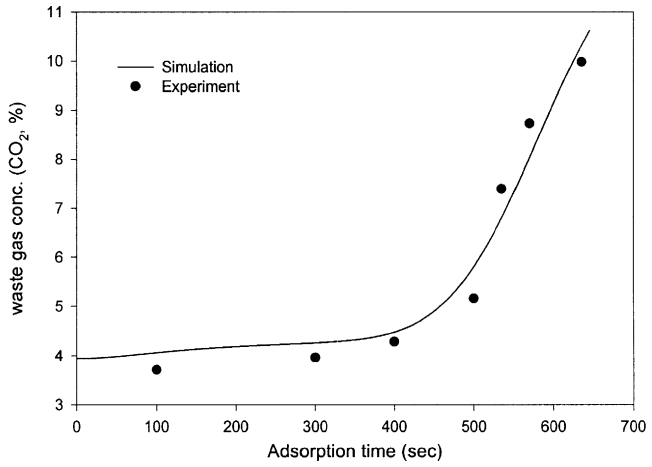

Fig. 3. Concentration changes of CO_2 at the product end of adsorption bed (pressure of adsorption: 1.5 atm).

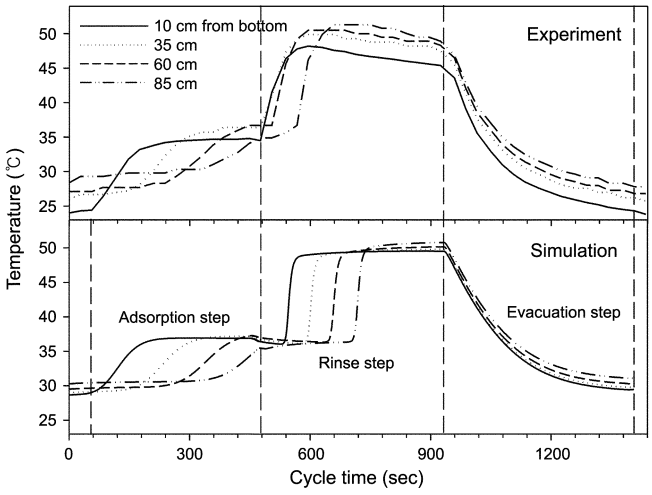

Fig. 4. Temperature profile in the adsorption bed (pressure of adsorption: 1.5 atm).

Analysis of temperature changes in the adsorption beds follows the analysis of CO_2 changes. Temperature changes are caused by heat of adsorption. From the temperature change we could identify the dynamic behavior of adsorption and desorption steps. Results of simulations for the temperature changes as well as those of experiments are shown in Fig. 4. Even with some discrepancy between simulations and experiments, the rates of increase and decrease of

temperatures in the adsorption and the desorption steps show good agreement with each other. In short, we can see that the PSA model developed in the present study can be effectively used to analyze the PSA process.

Results of numerical computations for the product purity and recovery as functions of the adsorption time and the reflux ratio are shown in Figs. 5-6. From these figures we can see that the recovery is inversely proportional to the adsorption step time at fixed reflux ratio. As the adsorption step time grew longer, the product purity was improved because the adsorption bed approached breakthrough and larger amount of CO_2 was adsorbed in the bed while the amount of waste CO_2 in the adsorption step was increased. The product purity was also improved even at short adsorption step time when the reflux ratio was fixed at relatively higher level regardless of the breakthrough in the adsorption step. On the contrary, the recovery was decreased due to higher reflux ratio. Thus, we can see that optimal choice of the adsorption step time and the reflux ratio affects the process performances seriously. Application of the optimal operating conditions identified in the present study (described in the next section) on experiments resulted in 99.5% purity and 69% recovery, and the simulation results based on optimal operating conditions were 99% purity and 65% recovery.

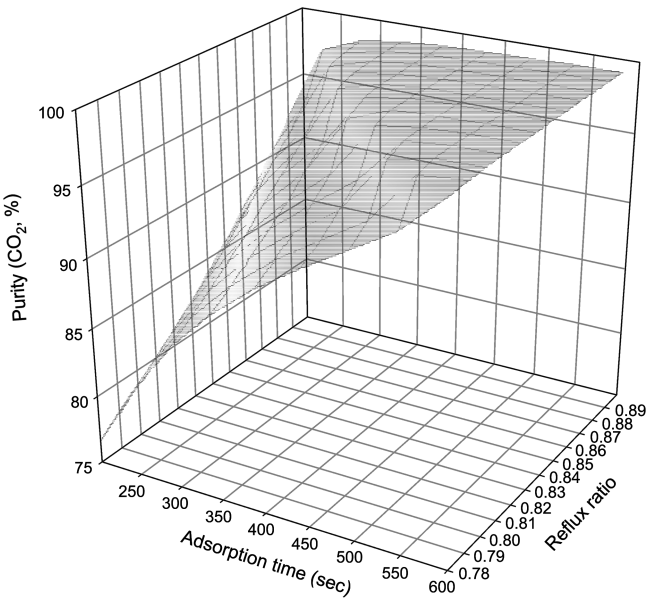

Fig. 5. Effects of the adsorption time and the reflux ratio on the purity.

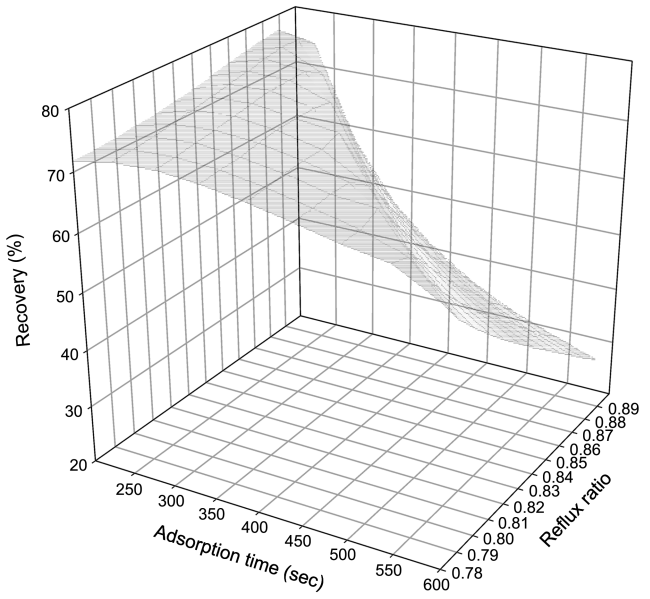

Fig. 6. Effects of the adsorption time and the reflux ratio on the recovery.

2. Optimization

Based on the numerical simulation results shown in Figs. 5-6, a set of nonlinear equations was obtained through nonlinear regression. From the nonlinear regression for the results shown in Fig. 5, we can obtain the objective function (9) as given below. The constraint can be obtained from the regression of the results shown in Fig. 6. In short, the optimization problem for the present study can be summarized as:

$$\text{Maximize } J = -1477.1 - 1.0066x_1x_2 + 0.7623x_1 + 3596.2856x_2 - 2043.6997x_2^2 \quad (9)$$

Subject to

$$-288.1326 + 0.1273x_1 + 753.8365x_2 - 0.0001x_1^2 - 401.6809x_2^2 \geq 90 \text{ (or } 95)$$
$$200 \leq x_1 \leq 600$$
$$0.77 \leq x_2 \leq 0.90$$

where x_1 is the adsorption step time and x_2 is the reflux ratio.

Well-known nonlinear optimization algorithms such as SQP (Sequential Quadratic Programming) method can be employed in the optimization. In the present study, the Matlab (v. 5.3) SQP algorithm contained in the optimization toolbox was used. Optimizations were performed for the cases when the product purity was

Table 6. Results of optimizations

Product purity (%)	Adsorption step time (sec)	Reflux ratio	Recovery (%)
Above 90	301	0.8288	78.01
Above 95	451	0.8005	72.53

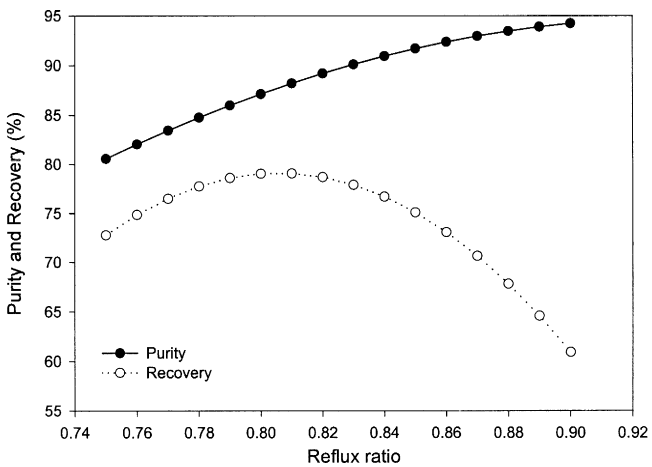

Fig. 7. Effects of the reflux ratio on the purity and the recovery (Product purity was above 90%).

above 90% and 95%. Results of optimizations are summarized in Table 6.

Figs. 7-10 show the effects of the reflux ratio and the adsorption step time on the product purity and recovery. In Fig. 7, when the adsorption step time was 301 sec and the reflux ratio was smaller than 0.8288 which is the optimal value, the purity was below 90% and the recovery was decreased. The feasible region for the recovery is [77, 90] at the reflux ratio of 0.8288. When the reflux ratio was larger than the optimal value, purity was more than 90% while the recovery grew worse. In Fig. 8, when the reflux ratio was 0.8288 and the adsorption step time was shorter than 301 sec, the recovery was improved while the purity was decreased below 90%. We can see that the feasible region for the recovery is [78, 90] at the reflux ratio of 0.8288. When the adsorption step time was longer than the optimal value, the purity was increased above 90% while the recovery grew worse.

In Fig. 9, when the adsorption step time was 451 sec and the reflux ratio was smaller than 0.8005 which is the optimal value, the recovery showed some improvement while the purity was below 95%. When the reflux ratio was larger than the optimal value, the purity was more than 95% but recovery grew worse. In Fig. 10, when the reflux ratio was 0.8005 and the adsorption step time was shorter than 451 sec, the recovery grew better while the purity was decreased below 95%. When the adsorption step time was longer than the optimal value, the purity was increased above 95% while the recovery grew worse.

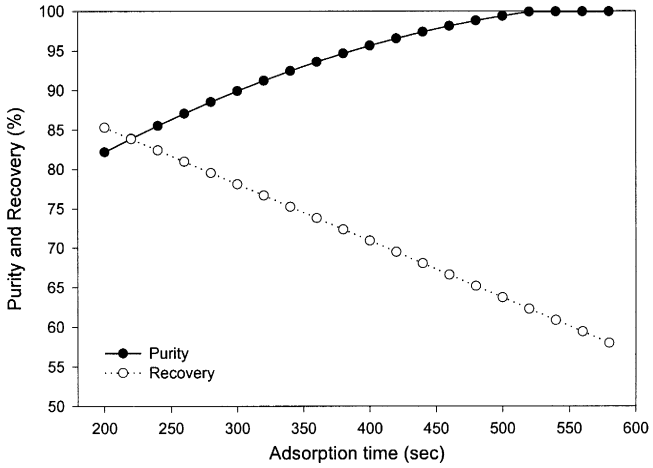

Fig. 8. Effects of the adsorption time on the purity and the recovery (Product purity was above 90%).

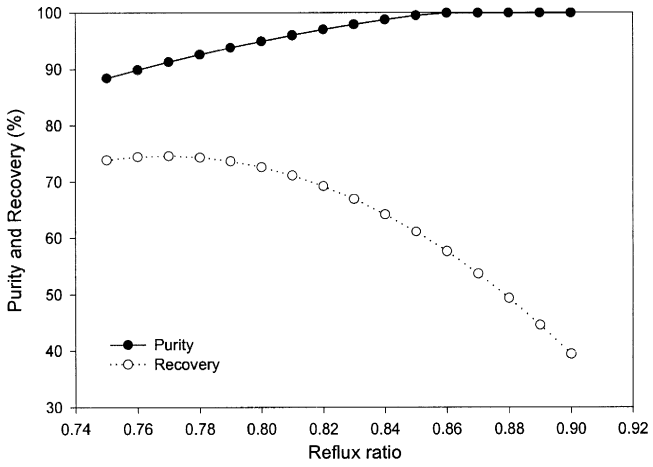

Fig. 9. Effects of the reflux ratio on the purity and the recovery (Product purity was above 95%).

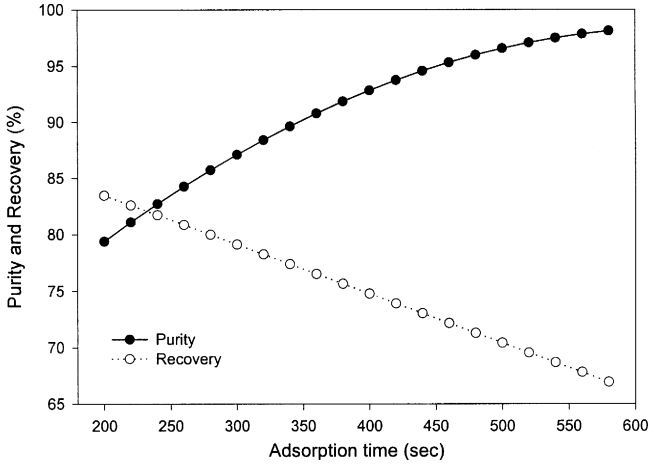

Fig. 10. Effects of the adsorption time on the purity and the recovery (Product purity was above 95%).

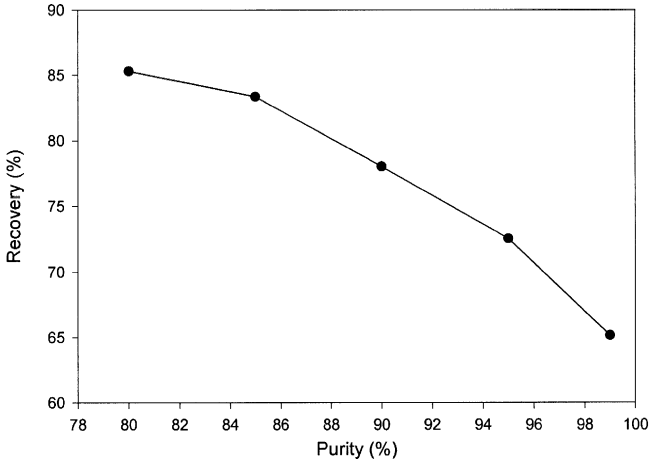

Fig. 11. Purity and recovery changes at optimal adsorption time and reflux ratio.

The relation between the recovery and the product purity at optimal operating conditions is shown in Fig. 11. This figure shows some inversely proportional relationship between the product purity and the recovery.

CONCLUSIONS

A PSA process for CO_2 separation and recovery was studied both experimentally and numerically. The model of the PSA process was developed based on the equilibrium adsorption isotherm experiment using pure CO_2 and N_2 gases and zeolite 13X. To verify simulation results, breakthrough curves and temperature changes in the bed were computed and compared with experimental results. The product purity and the recovery for each adsorption time and reflux ratio

were obtained through simulations. A set of nonlinear equations was obtained through nonlinear regressions based on the simulation results. The optimization problem was formulated based on these equations and SQP algorithm was employed to solve the nonlinear optimization problem. Optimal operating conditions were identified based on numerical simulations and were applied to experiments. The primary variables to be optimized in the present study were the adsorption step time and the reflux ratio. Investigation of other operating conditions in the PSA process will be the subject of the future research.

NOMENCLATURE

b_i : Langmuir parameter [atm^{-1}]
C_i : gas concentration of component i [mol/cm^3]
C_{total} : total gas phase concentration [mol/cm^3]
C_{ps} : heat capacity of adsorbent [J/g/K]
C_{pg} : specific heat of gas mixture [J/g/K]
ΔH_i : heat of adsorption of component i [KJ/mol]
k_i : overall mass transfer (LDF) rate coefficient of component i [s^{-1}]
L : bed height [cm]
q_i : amount adsorbed of component i on the solid phase [mol/g]
q_i^* : amount adsorbed of component I in equilibrium with gas phase [mol/g]
q_m : Langmuir parameter [mol/g]
R_g : gas constant [cm^3atm/gmol/K]
t : time [s]
t_1 : Langmuir parameter [mmol/g]
t_2 : Langmuir parameter [mmol/g K]
t_3 : Langmuir parameter [atm^{-1}]
t_4 : Langmuir parameter [K]
T : temperature [K]
u : interstitial gas velocity [cm/s]
z : position in the bed [cm]

Greek Letters

ρ_g : density of gas mixture [g/cm^3]
ρ_s : density of adsorbent [g/cm^3]
ρ_{bulk} : bulk density [g/cm^3]
ε : bed porosity [-]

REFERENCES

Chue, K. T., Kim, J. N., Yoo, Y. J., Cho, S. H. and Yang, R. T., "Comparison of Activated Carbon and Zeolite 13X for CO_2 Recovery from Flue Gas by Pressure Swing Adsorption," *Ind. Eng. Chem. Res.*, **34**, 591 (1995).

Farooq, S. and Ruthven, D. M., "Numerical Simulation of a Kinetically Controlled Pressure swing Adsorption Bulk Separation Process Based on a Diffusion Model," *Chem. Eng. Sci.*, **46**, 2213 (1991).

Kikkinides, E. S. and Yang, R. T., "Simultaneous SO_2/NO_x Removal and SO_2 Recovery from Flue Gas by Pressure Swing Adsorption," *Ind. Eng. Chem. Res.*, **30**, 981 (1991).

Kikkinides, E. S., Yang, R. T. and Cho, S. H., "Concentration and Recovery of CO_2 from Flue gas by Pressure Swing Adsorption," *Ind. Eng. Chem. Res.*, **32**, 2714 (1993).

Kim, Y. C., Yeo, Y. K., Lee, H. U., Song, H. K., Chung, Y. S. and Na, B. K., "Simulation of PSA Process for CO_2 Recovery from Flue Gas," *HWAHAK KONGHAK*, **36**, 562 (1998).

Moon, I. S., Lee, D. I., Yang, J. H. and Ryu, H. W., "Air Separation by Adsorption on Molecular Sieve 5A," *Korean J. Chem. Eng.*, **3**, 15 (1986).

Na, B. K., Koo, K. K. and Eum, H. M., "CO_2 Recovery from Flue Gas by PSA Process using Activated Carbon," *Korean J. Chem. Eng.*, **18**, 220 (2001).

Raghavan, N. S. and Ruthven, D. M., "Numerical Simulation of a PSA System," *AIChE J.*, **31**, 385 (1985).

Suzuki, M., "Adsorption Engineering," Elsevier, England (1990).

Yang, J., Park, M. W. and Chang, J. W., "Effects of Pressure Drop in a PSA Process," *Korean J. Chem. Eng.*, **15**, 211 (1998).

Yang, R. T. and Doong, S. J., "Gas Separation by Pressure Swing Adsorption: A Pore-Diffusion Model for Bulk Separation," *AIChE J.*, **31**, 1829 (1985).